Ionization and dissociation fractions of CO_2 under 10–30-keV H^-, C^-, and O^- negative-ion impact

Junqin Li,[1,2] Zilong Zhao,[1,2] Jingru Ye,[1,2] and Xuemei Zhang[1,2,*]

[1]*Institute of Modern Physics, Fudan University, Shanghai 200433, China*

[2]*Applied Ion Beam Physics Laboratory, Fudan University, Key Laboratory of the Ministry of Education, China*

(Received 30 July 2012; published 9 November 2012)

The ionization and dissociation fractions of the CO_2 molecule under the impact of 10–30-keV negative ions H^-, C^-, and O^- are studied. The four recoil ions originating from the target molecule CO_2 (CO_2^+, CO^+, O^+, and C^+) are measured and identified in coincidence with projectiles in two final charge states ($q = 0$ and $q = +1$) by using a time-of flight spectrometer. The ionization and dissociation fractions of CO_2 are found to associate with the momentum of the impacting ions. We also analyze the fractions for ionization and dissociation from a physical point. No comparison is given since no other experimental and theoretical data exist in the investigated energy range.

DOI: 10.1103/PhysRevA.86.052703 PACS number(s): 34.50.Fa, 34.70.+e

I. INTRODUCTION

Recently, the ionization and dissociation dynamics of molecules and atoms have attracted growing interest [1–9]. The total and partial ionization cross-section data are of practical importance in various fields, such as fusion-edge plasma diagnostics; gas discharge; planetary, stellar, and cometary atmospheres; radiation chemistry; and mass spectrometry, and in modeling radiation effects on materials including biomolecules [6]. In the above works [1–9], the cross sections for ionization and dissociation of some kinds of molecule and atom targets have been described very well for the impact of electrons, positive ions, and negative ions. However, these data for the cross sections of ionization and dissociation of molecule and atom targets are still very scarce, in particular, for the impact of negative ions which is only given in Refs. [3–5] for B, C, O, and F anions.

Negative ions, and especially their collision processes with molecules, play an important role in a number of areas, such as plasma physics, ionosphere physics, astrophysics, and flame chemistry. On the other hand, the ionization and dissociation cross-section data for atmospheric molecules, in particular for CO_2, are very important for a variety of reasons. Primarily, it is one of the fundamental constituents of planetary atmospheres. In view of this scenario, it is necessary and worthwhile to acquire reliable experimental data for ionization and dissociation cross sections of the CO_2 molecule induced by anions and to study the details of the collision dynamics of the fragmentation of this molecule. The different, and sometimes important, characteristics of anions may be helpful in the research of the dissociation dynamics of ionized molecules.

In the present work, we measure the ionization and dissociation fractions for the fragment ions of CO_2 induced by the impact of 10–30-keV H^-, C^-, and O^-. The four recoil ions originating from the target molecule CO_2 (CO_2^+, CO^+, O^+, and C^+) are measured and identified in coincidence with projectiles in two final charge states ($q = 0$ and $q = +1$) by using a time-of flight (TOF) spectrometer. Also we analyze the fractions for ionization and dissociation from a physical point. No comparison is given since no other experimental and theoretical data exist in the investigated energy range.

II. EXPERIMENTAL APPARATUS AND TECHNIQUE

Figure 1 shows the apparatus used for studying ionization and dissociation processes in negative ion-gas collisions. It has been described in detail in our previous work [10]. Here, we give a brief description of the apparatus. Negative ions produced by a cesium-sputtered negative-ion source (CSNIS) are analyzed by a 90° bending magnet according to their mass-to-charge ratio and then are focused and collimated to enter the collision chamber. In the chamber, the projectiles are made to cross a gas beam effusing from a grounded hypodermic needle at right angles, with the detection system mutually perpendicular to them. The gas jet target and electric field direction of the TOF spectrometer are orthogonal to each other. After the collision, the neutrals or positive ions from the projectile anions are detected by the position sensitive delay-line detector, the anions that do not lose electrons are collected by a Faraday cup (FC), and the recoil ions are detected by the anode plate detector after passing through a TOF spectrometer with a homogeneous electronic field of 12 V/cm perpendicular to the detector plane. In our experiment, the ejected electrons are not yet detected. The gas flow is controlled by a reducing valve and a fine needle valve. A turbo molecular pump backed by a rotary pump is used to maintain the base pressure of the chamber at 1×10^{-7} Torr; typical working pressures are of the order of 1×10^{-6} Torr with gas load.

We set up a new data acquisition system which is different from the previous work [10]. The present data acquisition system is similar to the one described in Ref. [11]. Here, we give a detailed description. Figure 2 shows the present data acquisition system. As in our previous work, two microchannel plate (MCP) detectors are used in the experiments. One is a position-sensitive delay-line detector used as the projectile-ion detector, the other is a MCP detector with a plate anode which is used as the recoil-ion detector. After amplification and time discrimination, the signals x_1, x_2, y_1, and y_2 from the position-sensitive delay-line detector are sent into one input channel of a multihit time-to-digital converter (TDC). The signal of recoil ions from the anode plate detector is also sent into one input channel of the TDC. In addition, it is used as the trigger signal

*zhangxm@fudan.edu.cn

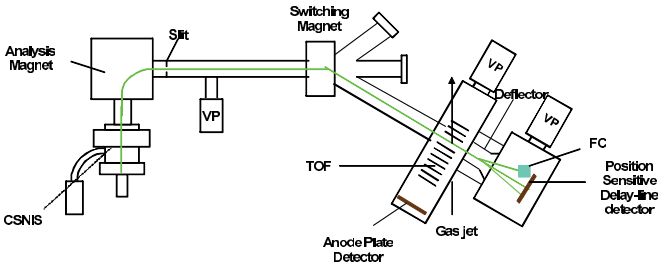

FIG. 1. (Color online) Schematic diagram of the experimental setup. CSNIS, VP, and TOF represent the Cs-sputtered negative-ion source, the vacuum pump, and the TOF mass spectrometer.

of the TDC after a delay of some microseconds. Finally, the time information of these five signals is stored and analyzed by self-developed data acquisition and process software. After analysis, TOF spectra of the recoil ions and position spectra of the projectile ions can be obtained. In current experiments, the TOF spectra of recoil ions are obtained in coincidence with projectiles in two final charge states ($q = 0$ and $q = +1$).

III. RESULTS AND DISCUSSION

By analysis of the TOF spectra of recoil ions, the fractions for ionization and dissociation of CO_2 targets under the impact of H^-, C^-, and O^- are obtained for two different final charge states of projectiles. This means that the fractions for ionization and dissociation of CO_2 are analyzed from the point of the final charge state of the projectiles. The process in which the projectiles are neutral is called the single-electron-loss (SL) channel. The process in which the projectiles are singly charged positive ions is called the double-electron-loss (DL) channel. The scattered ions are electrostatically analyzed and detected by the position-sensitive delay-line detector. Figure 3 gives the typical one-dimensional position spectrum of projectiles for a 20-keV H^- impact. Figure 4 shows the TOF spectrum of recoil ions of the SL channel for CO_2 targets under the impact of 30-keV H^-. As seen in Fig, 4, the most dominant

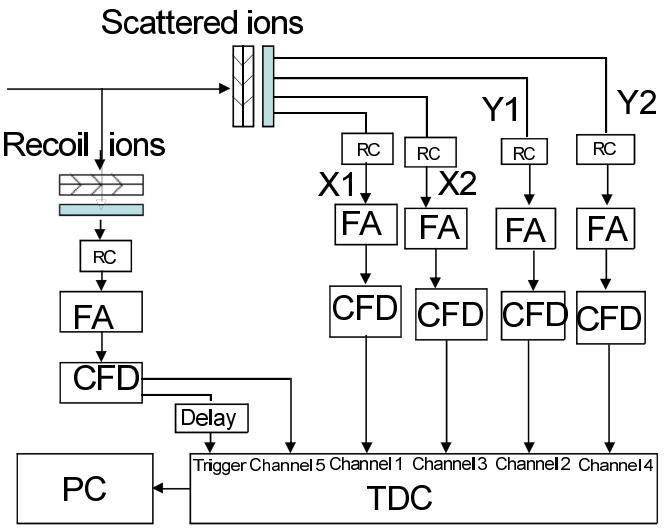

FIG. 2. (Color online) Data acquisition system. FA, fast amplifier; CFD, constant fraction discriminator; TDC, time-to-digital converter; RC, resistor-capacitor circuit; PC, personal computer.

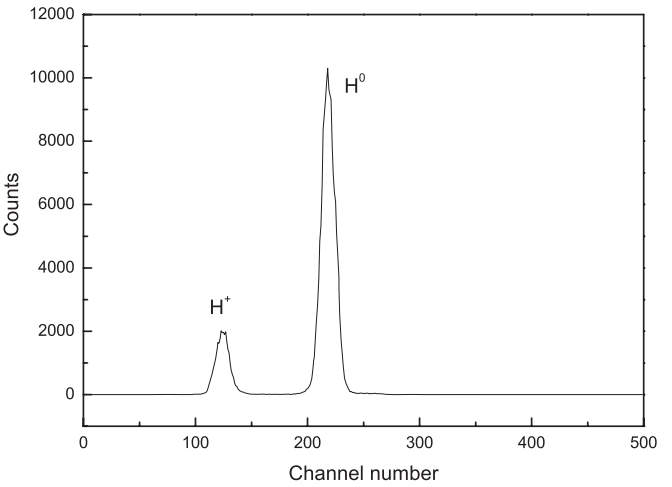

FIG. 3. A scattered ions position spectrum. After passing through the trumpet-shaped electric deflection plate, H^0 and H^+ ions are detected by the MCP position-sensitive detector, and H^- ions are collected by a Faraday cup.

peak corresponds to the $CO_2{}^+$ ions produced due to the direct ionization of CO_2 molecules. The peak $CO_2{}^{2+}$ is also from the direct ionization of CO_2 molecules. The fragment ions C^+, O^+, and CO^+ originate from the dissociative ionization of CO_2 molecules. In the present study, since it is difficult to completely resolve the fragment ions C^+ and O^+, as well as CO^+ and $O_2{}^+$, the computer fitting procedures are used to separate the peaks of C^+ and O^+ from H_2O^+ and of CO^+ from O_2^+ (see Fig. 4).

The possible dissociation channels after the multiple ionization of CO_2 are listed as follows [1]:

$$CO_2 \longrightarrow CO_2{}^+ + e \quad (1)$$
$$CO^+ + O \quad (1a)$$
$$O^+ + (C,O) \quad (1b)$$
$$C^+ + (O,O), \quad (1c)$$
$$CO_2 \longrightarrow CO_2{}^{2+} + 2e \quad (2)$$
$$C^+ + O^+ + O \quad (2a)$$

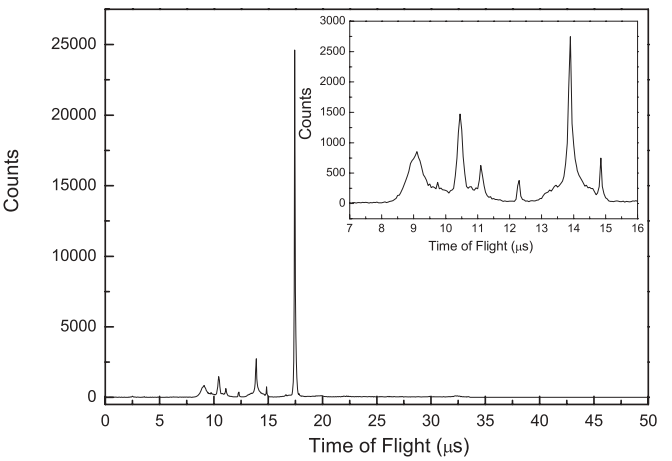

FIG. 4. TOF spectrum of recoil ions formed by a 30-keV H^- impact on CO_2.

$$2O^+ + C \quad (2b)$$
$$O^+ + CO^+ \quad (2c)$$
$$C^{2+} + (O,O) \quad (2d)$$
$$O^{2+} + (C,O). \quad (2e)$$

Multihit measurements were performed to look for the double- and triple-ionization channels and their fragmentation channels. It was found that there are not two or more charged ions produced in one event. Thus we rule out the channels (2a)–(2e) and the fragmentation channels of CO_2^{3+}. In addition, although there is a well-defined CO_2^{2+} peak in the spectrum, the count of CO_2^{2+} ions is so few that it cannot be analyzed well. No triply charged CO_2^{3+} ions have been observed experimentally. Here, we only analyze the ionization and dissociation fraction of channels (1a)–(1c).

With the above analysis, it can be known that CO^+, O^+, and C^+ come from only channels (1a), (1b), and (1c), respectively. Therefore, the factions for ionization and dissociation can be expressed by [10]

$$F(x) = \frac{N(x)/\epsilon(x)\eta(x)}{N(CO_2^+)/\epsilon(CO_2^+)\eta(CO_2^+)}, \quad (3)$$

where x represents the fragment ions of CO_2^+ (C^+, O^+, and CO^+), $F(x)$ is the ionization and dissociation fractions of channels (1a)–(1c), ϵ is the detection efficiency of the MCP for recoil ions, η is the collection efficiency of the TOF spectrometer for recoil ions, and N is the number of recoil ions. For the detection efficiency of the MCP for ions, $\varepsilon(CO_2^+)/\varepsilon(x)$ is considered as 1 within an error of about 5% in the present energy of recoil ions of 4 keV [12,13]. As discussed in our previous work [10], it is considered that all recoil ions are extracted and transported to the detector, and $\eta(CO_2^+)/\eta(x)$ is considered as 1 within an error of about 3.6%. In addition, due to peak fitting procedures, an additional error arises for C^+, O^+, and CO^+ ions within a few percent. Finally, the peaks of CO^+ and N_2^+ cannot be resolved by fitting procedures. We measured the TOF spectrum of the background. It was found that the count of N_2^+ is about 34% of the count of H_2O^+. Then it could be deduced that the count of N_2^+ is about 4.6% of the count of (CO^++ N_2^+). Here, we consider the contribution of N_2^+ as the error.

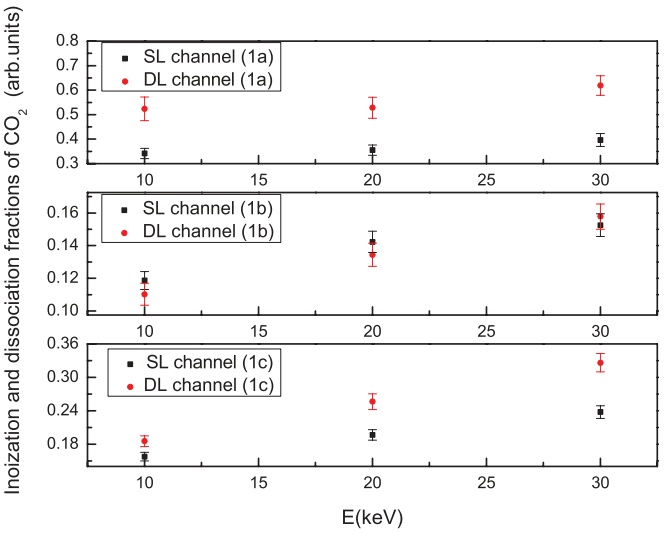

FIG. 5. (Color online) The ionization and dissociation fractions of CO_2 under the H^- impact.

The ionization and dissociation fractions of CO_2 for channels (1a)–(1c) and their total errors are presented in Table I for 10–30-keV H^-, C^-, and O^-negative-ion impact. In order to see more clearly, the fractions are also plotted in Figs. 5–7 for the impact of H^-, C^-, and O^-, respectively.

From Figs. 5–7, we can see that the ionization and dissociation fractions for channels (1a)–(1c) are almost energy dependent for both SL and DL processes for certain negative-ion impact. With increasing energy, the ionization and dissociation fractions for channels (1a)–(1c) increase except for the (1a) channel for both SL and DL processes and the (1b) channel for the SL process under C^- impact.

From Figs. 5–7, we can also see that the ionization and dissociation fractions for the DL process are larger than those for the SL process for certain energies and anion impact. As mentioned in our previous work [10], the DL process is preferred for small impact parameters in collision processes. This means that the DL process requires more energy loss, i.e., more violent collisions where the impact parameters are smaller and the momentum transfer is larger. Under the small impact parameters, more momentum is transferred to

TABLE I. The ionization and dissociation fractions of CO_2 under the impact of E = 10–30-keV H^-, C^-, and O^-.

		The ionization and dissociation fractions (arb. units)					
		SL			DL		
Impact ions	E (keV)	(1c)	(1b)	(1a)	(1c)	(1b)	(1a)
	10	0.157 ± 0.008	0.119 ± 0.005	0.342 ± 0.021	0.185 ± 0.010	0.110 ± 0.006	0.524 ± 0.048
H^-	20	0.197 ± 0.009	0.142 ± 0.006	0.355 ± 0.021	0.256 ± 0.014	0.134 ± 0.007	0.528 ± 0.043
	30	0.238 ± 0.011	0.153 ± 0.007	0.397 ± 0.026	0.326 ± 0.016	0.158 ± 0.008	0.619 ± 0.040
	10	0.112 ± 0.006	0.138 ± 0.007	0.703 ± 0.035	0.217 ± 0.012	0.196 ± 0.011	0.903 ± 0.045
C^-	20	0.271 ± 0.014	0.210 ± 0.012	0.963 ± 0.049	0.542 ± 0.027	0.593 ± 0.031	1.271 ± 0.063
	30	0.354 ± 0.018	0.176 ± 0.011	0.953 ± 0.048	0.860 ± 0.041	0.826 ± 0.046	1.228 ± 0.061
	10	0.126 ± 0.007	0.130 ± 0.008	0.665 ± 0.033	0.321 ± 0.018	0.266 ± 0.016	0.897 ± 0.044
O^-	20	0.373 ± 0.022	0.221 ± 0.018	1.198 ± 0.060	1.030 ± 0.049	0.808 ± 0.047	1.550 ± 0.077
	30	0.534 ± 0.039	0.344 ± 0.026	1.359 ± 0.069	1.467 ± 0.069	1.368 ± 0.080	1.769 ± 0.088

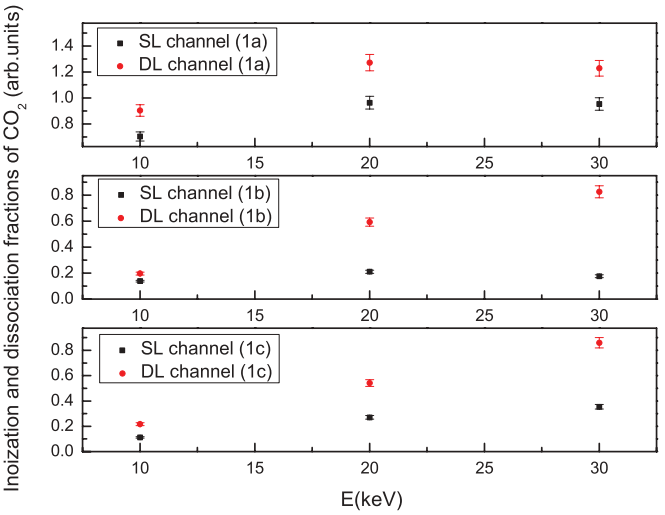

FIG. 6. (Color online) The ionization and dissociation fractions of CO_2^+ under the C^- impact.

the target. Thus, larger ionization and dissociation fractions are obtained for DL processes. The data show that this is the general case for these negative-ion projectiles.

From Figs. 5–7, we can still see that for certain impact energies, the fractions under the impact of anions with larger mass are larger than those under the impact of anions with smaller mass. Larger mass means more momentum if these anions have the same impact energy. In Fig. 8, we give the curve of the fractions as a function of the momentum of the impacting negative ions. It seems the fractions increase with increasing projectile momentum, independent of the projectile type. The ionization and dissociation fractions for the DL process increase more quickly than those for the SL process. Therefore the dissociation process is associated with the momentum of impacting ions as shown in Fig. 8. Further investigations are currently in progress.

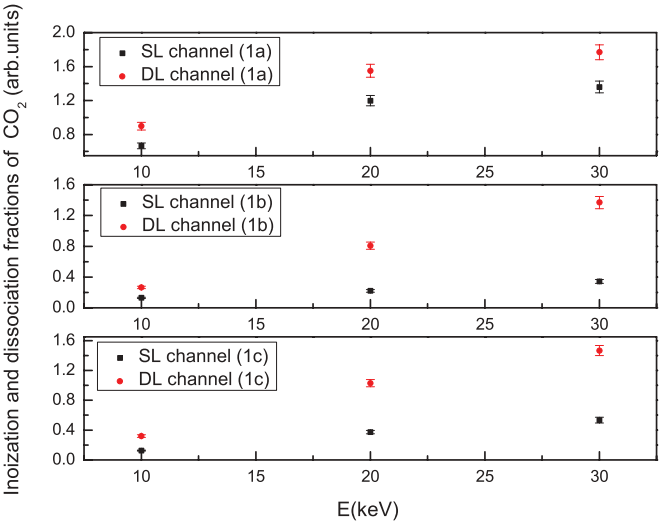

FIG. 7. (Color online) The ionization and dissociation fractions of CO_2^+ under the O^- impact.

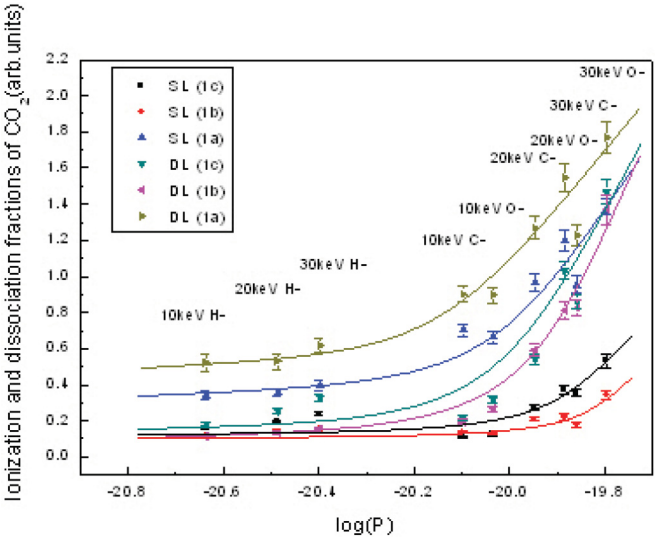

FIG. 8. (Color online) The ionization and dissociation fractions of CO_2 as a function of the momentum of impacting anions. The momentum P is in kg m/s. The points from left to right represent 10-keV H^-, 20-keV H^-, 30-keV H^-, 10-keV C^-, 10-keV O^-, 20-keV C^-, 20-keV O^-, 30-keV C^-, and 30-keV O^-, respectively.

IV. CONCLUSION

We obtained the ionization and dissociation fractions for the production of the fragment ions of CO_2 induced by the impact of 10–30-keV H^-, C^-, and O^-. The four recoil ions originating from the target molecule CO_2 (CO_2^+, CO^+, O^+, and C^+) were detected and identified in coincidence with projectiles in two final charge states ($q = 0$ for the SL process and $q = +1$ for the DL process) by using a TOF spectrometer. The ionization and dissociation fractions for channels (1a)–(1c) are expressed as formula (3). The ionization and dissociation fractions for channels (1a)–(1c) are almost energy dependent for both SL and DL processes for certain negative ions. It was also found that the ionization and dissociation fractions for the DL process occurring for small impact parameters are larger than those for the SL process occurring for large impact parameters. It was still found that the dissociation process may be associated with the momentum of impacting ions. We also analyzed the ionization and dissociation fractions from a physical point. No comparison is given since no other experimental and theoretical data about the ionization and dissociation of CO_2 exist under the impact of negative ions in the investigated energy range.

ACKNOWLEDGMENTS

We acknowledge Xincheng Wang for his help in building the new data acquisition system. This work is supported by the Chinese National Science Foundation (Grants No.10774026 and No. 10904019), the Program for New Century Excellent Talents in University (NCET), and the Shanghai Leading Academic Discipline Project, Project No. B107.

[1] C. Tian and C. R. Vidal, Phys. Rev. A **58**, 3783 (1998).
[2] B. G. Lindsay, M. A. Mangan, H. C. Straub, and R. F. Stebbings, J. Chem. Phys. **112**, 9404 (2000).
[3] F. Zappa, A. L. F. de Barros, L. F. S. Coelho, G. Jalbert, S. D. Magalhaes, and N. V. de Castro Faria, Phys. Rev. A **70**, 034701 (2004).
[4] A. L. F. de Barros, S. Martinez, F. Zappa, S. Suarez, G. Bernardi, G. Jalbert, L. F. S. Coelho, and N. V. de Castro Faria, Phys. Rev. A **72**, 032708 (2005).
[5] M. M. Sant Anna, F. Zappa, A. C. F. Santos, L. F. S. Coelho, W. Wolff, A. L. F. de Barros, and N. V. de Castro Faria, Phys. Rev. A **74**, 022701 (2006).
[6] P. Bhatt, R. Singh, N. Yadav, and R. Shanker, Phys. Rev. A **82**, 044702 (2010).
[7] M. R. Jana, P. N. Ghosh, B. Bapat, R. K. Kushawaha, K. Saha, I. A. Prajapati, and C. P. Safvan, Phys. Rev. A **84**, 062715 (2011).
[8] P. Bhatt, R. Singh, N. Yadav, and R. Shanker, Phys. Rev. A **84**, 042701 (2011).
[9] P. Bhatt, R. Singh, N. Yadav, and R. Shanker, Phys. Rev. A **85**, 034702 (2012).
[10] Z. Zhao, J. Li, and X. Zhang, Nucl. Instrum. Methods Phys. Res., Sect. B **283**, 35 (2012).
[11] X. Wang, B. Wei, Y. Shen, J. Xiao, X. Zhang, and Y. Zou, Nucl. Sci. Tech. **20**, 51 (2009).
[12] J. Oberheide, P. Wilhelms, and M. Zimmer, Meas. Sci. Technol. **8**, 351 (1997).
[13] N. Takahashi, S. Hosokawa, M. Saito, and Y. Haruyama, Phys. Scr. T **144**, 014057 (2011).